文章编号:1671-8879(2017)04-0012-06

Modeling of the temperature field during drifting of transport tunnels in cryolithic zone

ISAKOV A, GUDKOVA I

(Department of Survey, Design, and Construction of the Railways and Roads, Siberian State University of Railway Engineering, Novosibirsk 630049, Siberian, Russia)

Abstract: A mathematical model and algorithm for solving axisymmetric problems associated with determining the transient thermal field around a cylindrical stonedrift were described. A distinctive feature of the proposed model was introducing an air thermal boundary layer at the contact with the inner boundary of stonedrift in the formulation of the problem. The algorithm for this model was tested by calculating the thawing depth in a rock massif located in permafrost zone in the Far Eastern Part of Russia. The results show that these calculations yielded the thawing depth, which depends upon the thickness of heat insulating layer outside the tunnel lining. The article also presents the results for calculating the thawing depth for a rock mass along the tunnel's length when both sides of the tunnel are excavated. 6 figs, 10 refs.

Key words: tunnel engineering; cryolithic zone; rock thawing; thermal boundary layer; heat equation

CLC number: U419.92 **Document code**: A

冻土带交通隧道开挖期间的温度场模拟

ISAKOV A, GUDKOVA I

(西伯利亚铁路工程大学 道路与铁道勘测设计与施工系,西伯利亚州 新西伯利亚 630049)

摘 要:提出一种用于解决圆柱形岩石巷道轴对称问题和确定其周围瞬时温度场的数学模型和算法,该方法的显著特征是在岩巷内沿与大气的接触面上引入空气热边界层。通过计算位于俄罗斯远东多年冻土区某实际岩体的融化深度,对该算法及模型进行了验证。研究结果表明:该方法计算所得岩层融化深度取决于隧道衬砌外侧的隔热层厚度,同时还给出了双侧开挖施工后沿隧道长度方向上岩体融化深度的计算结果。

关键词:隧道工程;冻土带;岩体解冻;热边界层;热方程

0 Introduction

Creating transport tunnels into cryolithic zones has several problems, among which include the thawing of strata that results in a stability loss for stonedrift arches, and allows groundwater penetration into the tunnel. Thus, it is very important that, during tunnel construction design, the dy-

Received date: 2017-03-03

Author resume: ISAKOV A, Professor, PhD, E-mail:mylab@ngs.ru.

namics data for permafrost degradation around the stonedrift is available, but sometimes, even this data is insufficient. It is more important to control this process to effectively protect a tunneling from groundwater penetration. Furthermore, it is impossible to model the change in soil's permafrost temperature around the stonedrift without mathematical modeling. Numerous papers are devoted to the prognosing the temperature field, which occurs during mining work in the cryolitic zones. For instance, Khokholov, et al.[1], Soloviev, et al.[2], and Galkin, et al.[3], among others, used different semi-empirical dependencies to model the heat exchange between a tunnel's inner surface and the air flow inside the tunnel. In this case, the tunnel's surface temperature was assumed to be constant throughout its cross section, as well as the air stream's temperature. But in reality, the tunnel's surface temperature changes in real time.

In the present paper, a model and an algorithm are provided to solve axially symmetric problems that determine the non-stationary, thermal field around cylindrical stonedrifts, where the heat exchange between the tunnel surface and the circulating air flow inside are accounted for, by introducing a thermal boundary layer into the model. In this approach, changes in tunnel's surface temperature will be accounted as a function of time, even when the air stream temperature is constant.

1　Formulation of the problem

The massif area surrounding the cylindrical stonedrift possesses a diameter D_0 (Fig. 1), and is divided along its radius into separate tubular elements with singular lengths equal to the wall thickness (Fig. 2). The air mass circulating in the tunnel has a preset function describing the temperature change $T_{air}(t)=F(t)$, which is separated from the inner lining by the air's thermal boundary layer with thickness δ. At the instantaneous time t of $t=0$, the function describes the temperature field for N elements in the environment. Temperature of the N-th element, with a distance of zero year amplitudes from the cavity boundary, is constant in time, and is equal to T_0. The temperature distribution for every element in the environment must be determined for a random value of time t.

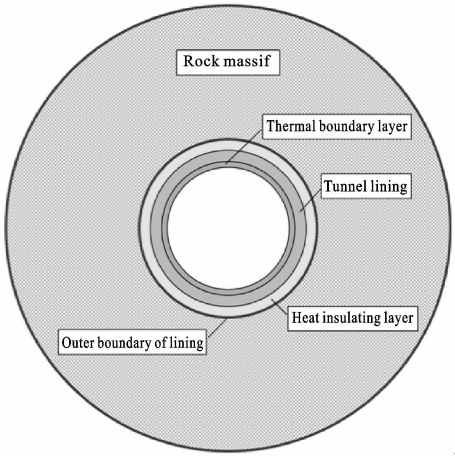

Fig. 1　Schematic of tunnel lining layers and rocks of surrounding massif

图 1　隧道衬砌层及围岩示意

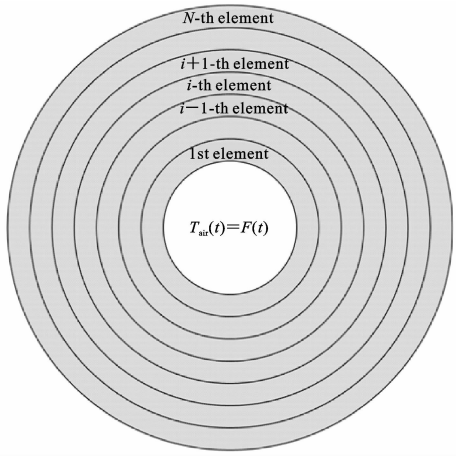

Fig. 2　Diagram illustrating the discrete model representing the problem

图 2　离散模型图示

The formulated problem assumes that heat flow is spread only in radial directions throughout the entire space, e. g., as a one-dimensional model[4]. Another commonly accepted assumption is that air flow circulating in the tunnel is stationary, i. e., air speed in every layer is assumed to be a function of only the distance from the tunnel lining's inner boundary. Then, the thickness of

thermal boundary layer δ can be estimated, using a certain degree of approximation, following to Buhmirov, et al.[5]

$$\delta \approx \frac{D_0}{\sqrt{PrRe}} \tag{1}$$

where $Pr=\nu/a$ is Prandtl number; $Re=D_0V_0\rho_{air}/\mu$ is Reynolds number; V_0 is average air flow speed inside the tunnel; ν is kinematic coefficient of viscosity; μ is dynamic viscosity; a is thermal diffusivity (m^2/s); ρ_{air} is the air density (kg/m^3).

2 Algorithm of the problem

As mentioned in previous section, the model is represented with tubular elements[6]. The dimensions of i-th element: Δh is thickness of the i-th element boundary layer; $2\pi R_{i-1}$ and $2\pi R_i$ describe the lengths of inner and outer boundaries, respectively, where $R_i=R_0+i\Delta h$, R_0 is the inner radius of the tunnel. The square of inner and outer surfaces are denoted as $S_{i,0}=2\pi R_{i-1}$ (m^2) and $S_{i,1}=2\pi R_i$ (m^2), respectively. In such a case the quantity of heat ΔQ_i yielded or received from outside by i-th element during time interval Δt, may be expressed as follow

$$\Delta Q_i=(J_{i-1}S_{i,0}-J_{i+1}S_{i,1}\Delta t) \tag{2}$$

where J_{i-1} represents heat flow, transferred through the unit of area from the i-th to the $(i-1)$-th element during a unit of time, $i=1,2,\cdots,N$, as shown in Fig. 2, Eq. (3); J_{i+1} describes the heat flow transferred through the unit of area from the $(i+1)$-th element to the i-th element during a unit of time

$$J_{i-1}=\lambda_{i-1}\frac{T_{i-1}(t)-T_i(t)}{\Delta h} \tag{3}$$

$$J_{i+1}=\lambda_i\frac{T_i(t)-T_{i+1}(t)}{\Delta h} \tag{4}$$

where λ_i is heat conductivity coefficient for the i-th element [W/(m·℃)].

The law of energy conservation for the i-th element may be written as follow

$$\Delta Q_i=m_iC_i[T_i(t)-T_i(t+\Delta t)]+Q_{ph}m_i\big|_{T=T_{ph}} \tag{5}$$

where $m_i=\pi\rho_i(R_i^2-R_{i-1}^2)$ is mass of the i-th element; ρ_i is density of the i-th element (kg/m^3); Q_{ph}, T_{ph} are the phase transition temperature and heat, which describe freezing-up of the liquid in soil.

When substituting Eq. (2) to Eq. (4) into Eq. (5), the temperature of the i-th element at time increment $t+\Delta t$ is determined by Eq. (6)

$$T_i(t+\Delta t)=T_i(t)+2a_i\left\{\frac{\lambda_{i-1}}{\lambda_i}[T_{i-1}(t)-T_i(t)]R_{i-1}-[T_i(t)-T_{i+1}(t)]R_i\right\}\cdot\frac{\Delta t}{\Delta h(R_i^2-R_{i-1}^2)}+\frac{Q_{ph}(\Delta t)}{C_i}\Bigg|_{T=T_{ph}} \tag{6}$$

where $a_i=\lambda_i/(\rho_iC_i)$ is thermal diffusivity of the i-th element; C_i is specific heat of the i-th element [J/(kg·℃)].

Heat exchange between the thermal boundary layer and the tunnel's inner surface is described by the equation of energy conservation by analogy with Eq. (7)

$$T_1(t+\Delta t)=T_1(t)+2a_i\left\{\frac{\lambda_{air}}{\lambda_1}[T_{air,1}(t)-T_1(t)]R_0-[T_1(t)-T_2(t)]R_1\right\}\cdot\frac{\Delta t}{\Delta h(R_1^2-R_0^2)}+\frac{Q_{ph}(\Delta t)}{C_1}\Bigg|_{T=T_{ph}} \tag{7}$$

where $T_1(t)$ is the temperature of tunnel's inner surface (℃); $T_{air,1}(t)$ is the temperature of the 1st element in air's boundary layer (℃); λ_{air} is heat conductivity coefficient for air [W/(m·℃)].

Heat exchange between inner elements of air's boundary layer is determined by analogy with Eq. (6)

$$T_{air,i}(t+\Delta t)=T_{air,i}(t)+2a_{air}\{[T_{air,i-1}(t)-T_{air,i}(t)]R_{air,i-1}-[T_{air,i}(t)-T_{air,i+1}(t)]R_{air,i}\}\frac{\Delta t}{\Delta h(R_{air,i-1}^2-R_{air,i}^2)} \tag{8}$$

where $a_{air}=\lambda_{air}/(\rho_{air}C_{air})$ is thermal diffusivity of air, and C_{air} is specific heat capacity of air [J/(kg·℃)].

Soil's thermal and physical characteristics are determined by its moisture content, and by the aggregative state of water contained within the soil, where $\rho=\rho_s(1+W)/(1+e)$ is soil density (kg/m^3),

W represents the moisture in soil; is density of soil hard particles (kg/m^3), e is void ratio.

$$C_{th}=(C_s+WC_{air})/(1+W)$$

where C_{th} represents the specific heat capacity of the thawed soil, C_s is the specific heat of soil's hard particles.

$$C_{fr}=[C_s+(W-W_{un})C_{ice}+W_{un}C_w]/(1+W)$$

where C_{fr} is specific heat capacity of frozen soil.

$$W_{un}=k_wW_p$$

where W_{un} represents the unfrozen fraction of water in the soil; W_p represents the plastic limit of the soil; k_w is special coefficient depending on the type of the soil.

$$a_{th}=\lambda_{th}/(\rho C_{th})$$

where a_{th} is thermal diffusivity of thawed soil.

$$a_{fr}=\lambda_{fr}/(\rho C_{fr})$$

where a_{fr} is thermal diffusivity of frozen soil.

$$Q_{ph}=Q_{ice}(W-W_{un})/(1+W)$$

where Q_{ph} represents specific heat of soil's phase transition (J/kg), Q_{ice} is specific heat of ice fusion (J/kg), λ_{th} is the heat conductivity coefficient for thawed soil, λ_{fr} is the heat conductivity coefficient for frozen soil.

For each layer of N tubular elements, the temperature is defined with Eq. (6) using two cycles: first, increments in time and along radius are represented by Δt and Δh, respectively; and second, equations for heat exchange are used with the thermal boundary layer for air contained in Eq. (7) and Eq. (8). Note that this algorithm is based upon on the conservation of energy law, which should produce correct results.

3　Practical calculations

The algorithm in previous section was implemented in the computer program "Tube-1", which was designed at the Department of Survey, Design, and Construction of Railways and Roads in the Siberian State University of Railway Engineers[7-8]. The example given below is a heat engineering calculation for a tunnel designed for the cryolitic zone in the Far Eastern Part of Russia. A two-coat lining was chosen for this example. The inner layer consists of 0.5 m thick concrete, and the outer layer is composed of a heat insulating material with varied thickness. The soil's thermal and physical characteristics were entered into the program[9-10]:

① particle density;

② void ratio;

③ moisture content;

④ specific heat of soil's particles;

⑤ thermal conductivities for thawed and frozen soil.

The thermal and physical characteristics for the heat insulating material were also entered into the program:

① heat insulating material's density;

② moisture content;

③ specific heat;

④ thermal conductivity.

The soil behind the lining was assumed as granite with the following characteristics:

① the specific heat $C_{th}=0.7$ kJ/(kg·℃);

② the thermal conductivity $\lambda_{th}=2.0$ W/(m·℃).

In the presented model, air flow inside the tunnel is considered stationary during the entire time simulation, while the temperature is assumed to be a constant value of +10 ℃. Other boundary conditions also exist for the internal radius of the tunnel, the radius of the calculation zone, and the temperature of the surrounding mountain mass. In the presented calculations, the internal radius of the tunnel is 4 m, and the radius of the calculation zone is 30 m, while the temperature at this zone's boundary is −1.5 ℃, and is based upon a thermometric investigation.

If all other conditions are equal, the following factors affect the thawing depth of the surrounding mountain mass:

① temperature inside the tunnel;

② air flow speed;

③ mode of tunnel ventilation;

④ thickness of the heat insulation layer.

Referring to the algorithm, from Eq. (10), it is observed that the air flow speed V_0 influences the thermal boundary layer's thickness, which in turn, affects the intense heat exchange between the air flow and the tunnel wall's lining. Fig. 3 shows the change in thawing depth over one year, and is subject to the tunneling process, which depends upon the thermal boundary layer's thickness and the parameters cited above.

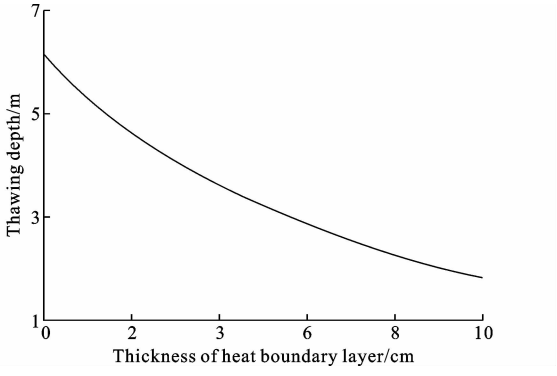

Fig. 3 Thawing depth as a function of the heat boundary layer's thickness over one year

图 3 一年中融化深度与热边界层厚度的关系

The most problematic variant is round-the-clock ventilation of the tunnel with an air temperature of +10 ℃. This is the minimum acceptable level at which personnel can operate comfortably during the tunneling process. In this case, the only way to decrease the massif's thawing zone is to introduce the heat insulation material into the tunnel lining during construction. Foamed polystyrene was used as the heat insulation material, and possessed the following characteristics:

① its density is 40 kg/m^3;

② its moisture content is 0.01;

③ its specific heat is 1 530 J/(kg · ℃$^{-1}$);

④ its coefficient of thermal conductivity is 0.035 W/(m · ℃).

In the subsequent calculations, the thickness of thermal boundary layer is taken as 2 cm, which is in accordance with Eq. (1), and the average air flow velocity is 0.4 m/s. As shown in Fig. 4, while the change in the massif's thawing depth versus time was measured for a fixed tunnel cross section with different thicknesses of foamed polystyrene.

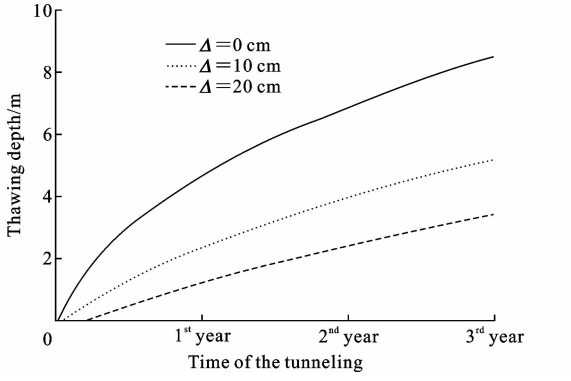

Fig. 4 Changes in massif's thawing depth with time under different thicknesses of heat insulation material (Δ)

图 4 不同保温材料厚度(Δ)下地层融化深度随相对时间的变化

Dynamics for the temperature changes in the lining's surface was measured for a fixed cross section with different thicknesses of heat insulation material as shown in Fig. 5.

In Fig. 6, calculation results for thawing depth behind the massif's lining along the tunnel are illustrated. Both sides are excavate with a tunneling speed of 30 m per month.

The results of thermometric measurements collected in the mountain massif, and around the constructed tunnel in the given climatic zone, where measurements were collected without an additional thermal insulation layer, show that the massif's thawing depth varies within the limits of 4 to 7 m, and is subjected to watering geological material.

4 Conclusions

(1) The simulation algorithm for heat exchange between the tunnel walls and the circulating air flow considers the thermal boundary layers and the dynamic temperature changes within the tunnel's internal walls.

(2) This algorithm reveals a more accurate thawing process for the surrounding mountain mass while

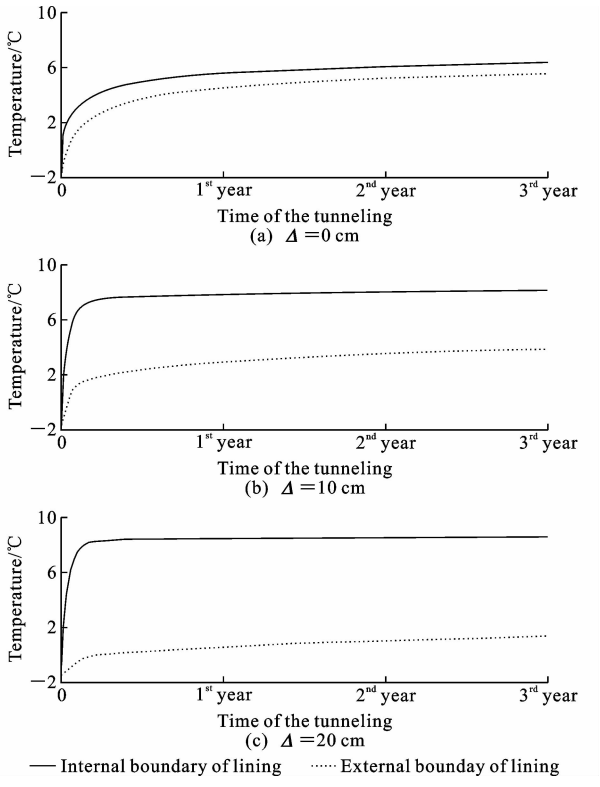

Fig. 5　Changes of internal and external boundaries temperatures of different thicknesses of heat insulation material of foamed polystyrene with time

图 5　不同厚度泡沫聚苯乙烯保温材料的内边界温度和外边界温度随时间的变化

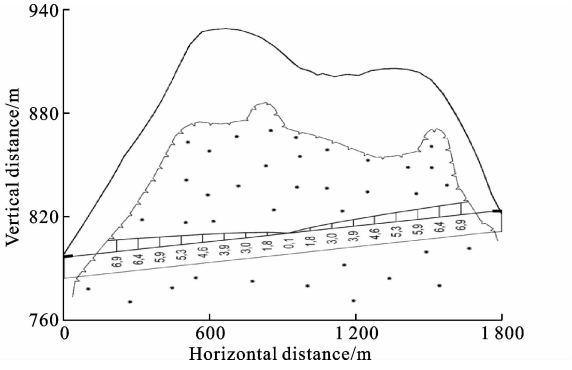

Fig. 6　Calculation results of thawing depth after both sides are excavated with a excavating speed of 30 m per month

图 6　开挖速度为 30 m/月双侧开挖后融化深度计算结果

it is drifting. The calculations show that the introduction of an additional thermal insulation layer, with a thickness of 20 cm, decreases the thawing zone of the mountain mass by 3 times, by the end of the first year of tunneling construction.

(3)By the end of the third year of tunnel construction, the maximum permafrost degradation varies along the tunnel from a cross section of 0 to 8 m, or to the working face along the edge sections. It is noteworthy that the air temperature is maintained at a constant value of +10 ℃.

References:

[1] KHOKHOLOV Y A, SOLOVIEV D E. Temperature regime in permafrost during underground mining[J]. Mining Information and Analytical Bulletin, 2009(4): 270-275.

[2] SOLOVIEV D E. Thermal regime of the mine during underground mining in cryolithic zone[J]. Young Scientist, 2011, 12(1): 53-55.

[3] GALKIN A F. Thermal control in the ore mines of cryolithic zone[J]. Metallurgical and Mining Industry, 2016(4): 24-27.

[4] ISAKOV A L, KIM K C. Thermal discrete model of soil freezing of roadbed[J]. Transport of the Ural, 2012, 2(33): 121-125.

[5] BUHMIROV V V, RAKUTINA D V. The study of heat transfer in the forced motion of air in a pipe by the method of imitating modeling[J]. Proceedings of Ivanovo State University of Energetics, 2014, 23: 1-13.

[6] KHOKHOLOV Y A, SOLOVIEV D E. Mathematical modeling of thermal processes in the mining processes of mines in the North[J]. Novosibirsk, 2013, 186: 1-12.

[7] HSIAO J S. An efficient algorithm for finite-difference analyses of heat transfer with melting and solidification[J]. Numerical Heat Transfer, 1985, 8(6): 653-666.

[8] KHOKHOLOV Y A, KURILKO A S. Mathematical simulation of thermal processes in underground/workings of mines located in the cryolithic zone[C]// IMVC. Eighth International Mine Ventilation Congress. Brisbane: IMVC, 2005: 467-470.

[9] GALKIN A F. Increase of stability of mine workings in the permafrost zone[M]. St. Petersburg: Mining Institute, 2014.

[10] SHUVALOV Y V, GALKIN A F. The theory and practice of optimal thermal management of underground facilities permafrost[J]. Mining Informational and Analytical Bulletin, 2010(8): 365-370.